JACS
JOURNAL OF THE AMERICAN CHEMICAL SOCIETY
pubs.acs.org/JACS
Article

A Case Study in Catalyst Generality: Simultaneous, Highly-Enantioselective Brønsted- and Lewis-Acid Mechanisms in Hydrogen-Bond-Donor Catalyzed Oxetane Openings

Daniel A. Strassfeld, Russell F. Algera, Zachary K. Wickens, and Eric N. Jacobsen*

Cite This: J. Am. Chem. Soc. 2021, 143, 9585–9594
Read Online
ACCESS | Metrics & More | Article Recommendations | Supporting Information

ABSTRACT: Generality in asymmetric catalysis can be manifested in dramatic and valuable ways, such as high enantioselectivity across a wide assortment of substrates in a given reaction (broad substrate scope) or as applicability of a given chiral framework across a variety of mechanistically distinct reactions (privileged catalysts). Reactions and catalysts that display such generality hold special utility, because they can be applied broadly and sometimes even predictably in new applications. Despite the great value of such systems, the factors that underlie generality are not well understood. Here, we report a detailed investigation of an asymmetric hydrogen-bond-donor catalyzed oxetane opening with TMSBr that is shown to possess unexpected mechanistic generality. Careful analysis of the role of adventitious protic impurities revealed the participation of competing pathways involving addition of either TMSBr or HBr in the enantiodetermining, ring-opening event. The optimal catalyst induces high enantioselectivity in both pathways, thereby achieving precise stereocontrol in fundamentally different mechanisms under the same conditions and with the same chiral framework. The basis for that generality is analyzed using a combination of experimental and computational methods, which indicate that proximally localized catalyst components cooperatively stabilize and precisely orient dipolar enantiodetermining transition states in both pathways. Generality across different mechanisms is rarely considered in catalyst discovery efforts, but we suggest that it may play a role in the identification of so-called privileged catalysts.

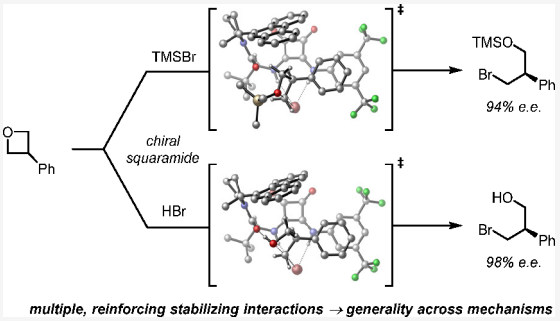

INTRODUCTION

The birth of the field of modern asymmetric catalysis can be tied to the discovery made over a half century ago that chiral small molecules can promote reactions of interest with very high, "enzyme-like" levels of enantioselectivity.[1] The practical and fundamental implications of such transformations became well-appreciated, fueling intensive research in the ensuing years that has produced a continuously expanding list of enantioselective catalytic organic reactions. A small subset of those reactions has proven to be remarkably accommodating of changes in substrate structure, enabling their broad application (e.g., Figure 1A).[2] The development of such reactions remains a challenging and rarely met objective, but from a conceptual standpoint, their generality can be rationalized fairly simply: in such processes, the chiral catalyst exerts precise geometric control on the prochiral reaction site, but selectivity does not rely on interactions with the variable substituents on the substrate.[3] Another, quite different type of generality emerged unexpectedly throughout the development of the field of asymmetric catalysis, wherein certain chiral scaffolds have proven to be effective at inducing high levels of enantioselectivity across a wide range of mechanistically unrelated reactions (e.g., Figure 1B).[4] These so-called privileged chiral catalysts or frameworks have proven enormously enabling for the discovery of new enantioselective, catalytic processes. Indeed, there are examples of extraordinarily useful new transformations[5] and new modes of catalysis[6] or new classes of reactions[7] that were developed with reliance on chiral frameworks which were identified previously for different purposes. Analysis of privileged chiral scaffolds identified to date has provided some insight into their common features: most notably, structural rigidity achieved through chelation of a ligand to a reactive metal center and C_2 symmetry to create stereochemically equivalent reactive sites.[4a,8] However, these characteristics are also common to many chiral frameworks that are not broadly applicable in asymmetric catalysis and are absent from several of the privileged frameworks that have been identified. Unfortunately, fuller elucidation of the structural features that underlie the privileged nature of such catalysts is confounded by the difficulty of studying systems that differ not only in mechanism but also in nearly every other

Received: April 15, 2021
Published: June 21, 2021

https://doi.org/10.1021/jacs.1c03992
J. Am. Chem. Soc. 2021, 143, 9585–9594

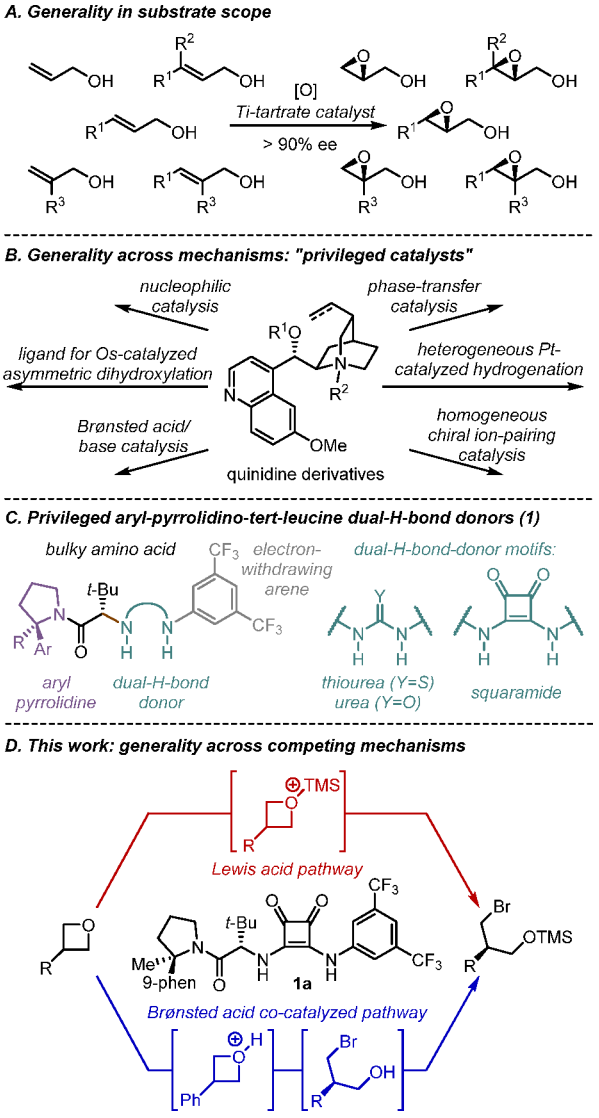

Figure 1. (A) The Sharpless epoxidation represents a prototypical example of substrate generality in an asymmetric catalytic reaction. Even though the reaction scope is limited to allylic alcohols, it tolerates extensive variation in the alkenyl substituents, thereby enabling its broad application in synthesis. (B) The cinchona alkaloids are prototypical privileged chiral frameworks for asymmetric catalysis. Such systems are capable of inducing high enantioselectivity across a range of mechanistically unrelated reactions (refs 4a, 10). (C) Dual H-bond donors containing an aryl-pyrrolidine-*tert*-leucine motif with the general structure **1** have emerged as a privileged class of chiral organocatalysts. (D) The addition of TMSBr to oxetanes catalyzed by chiral squaramide **1a** can proceed simultaneously by fundamentally different, yet highly enantioselective Lewis- and Brønsted-acid mechanisms.

key reaction parameter (e.g., identity of substrates, additives, and other reagents, solvents, temperature, etc.)

Over the past decade, thioureas, ureas, and squaramides with the general structure **1** (Figure 1C) have emerged as a privileged class of organocatalysts capable of inducing high levels of enantioselectivity in transformations proceeding through a variety of mechanisms, including ion-pairing catalysis involving nucleophilic addition to sp^2 and sp^3-hybridized cationic electrophiles, concerted nucleophilic substitution reactions, enantioseletive proton transfers, and direct activation of electrophiles via LUMO lowering.[9] As part of this body of work, we recently reported that squaramide **1a** catalyzes the highly enantioselective opening of a structurally diverse set of 3-substituted oxetanes with TMSBr (Figure 2A).[9l] Here, we report a detailed mechanistic investigation

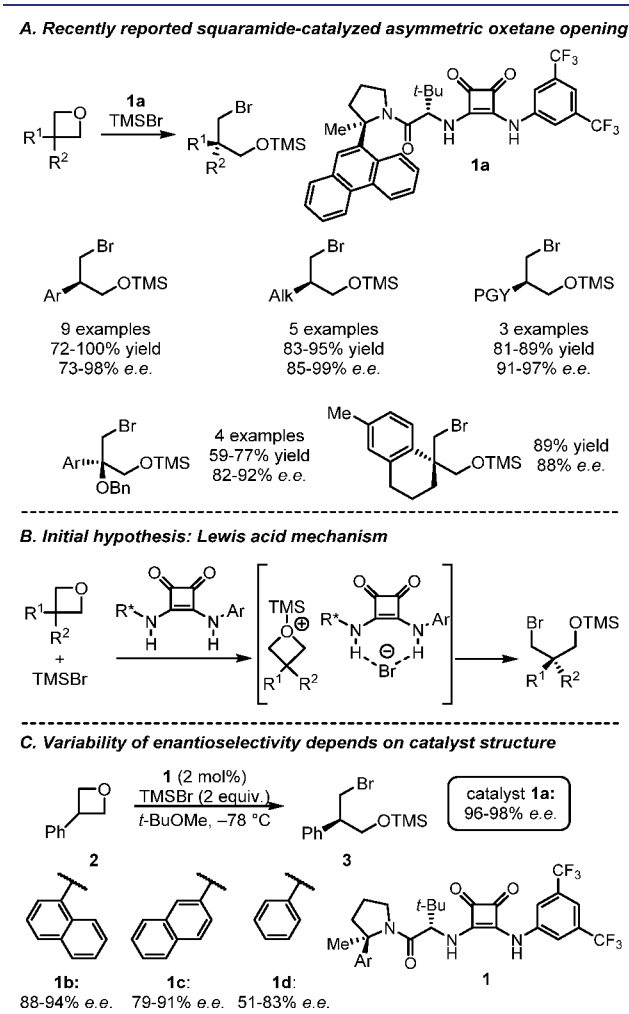

Figure 2. (A) Chiral squaramide-catalyzed addition of TMSBr to oxetanes (ref 9l). (B) Original mechanistic hypothesis for the oxetane ring-opening reaction. (C) Catalyst **1a** reproducibly affords highly enantioenriched products, but reactions catalyzed by other structurally similar H-bond donors fail to provide reproducible levels of enantioselectivity.

revealing that the reaction proceeds through competing Brønsted-acid and Lewis-acid mechanisms (Figure 1D), both of which contribute significantly to product formation under typical reaction conditions. The participation of multiple, highly enantioselective reaction channels leading to the same enantiomer of product in a single transformation provided an opportunity to study the catalyst features that underlie mechanistic generality without the confounding variables that typically hinder such comparisons. Analysis of the mechanism of stereoinduction in the competing pathways revealed the engagement of colocalized, reinforcing secondary interactions that cooperatively stabilize the transition state leading to the major enantiomer of product in both mechanisms. We advance that the presence of such reinforcing sites may be a common feature in privileged catalysts that operate via attractive noncovalent interactions.

https://doi.org/10.1021/jacs.1c03992
J. Am. Chem. Soc. 2021, 143, 9585−9594

RESULTS AND DISCUSSION

Earlier studies from our lab established that chiral squaramide derivatives capable of dual H-bond-donor interactions promote heterolysis of silyl triflates via anion abstraction and activate the resulting electrophile-triflate ion-pairs through anion-binding catalysis.[9e,h,11] We initially reasoned that a similar Lewis-acid-activation mechanism could be operative in the oxetane-opening with TMSBr (Figure 2B).[9l] However, observations made during the development of that reaction provided compelling evidence that this proposal was at best incomplete. In particular, the rate of the reaction was found to decrease quite dramatically with increasing scale (Figure S4), an effect that could not be ascribed simply to changes in mass transport given the homogeneous nature of the reaction mixtures. Additionally, an important difference was observed between the behavior of optimal catalyst **1a** and other chiral squaramide dertivatives in the same family: the reaction catalyzed by **1a** afforded product **3** with reproducibly high levels of enantioselectivity (e.e.), whereas suboptimal catalysts such as **1b**-**1d** afforded product with highly variable e.e.'s (Figure 2C).

The hydrolysis of Lewis acids or metal salts to yield Brønsted acids as potentially active reagents is well documented in racemic chemistry[12,13] and has also been considered in the context of asymmetric catalysis.[14−18] One example directly relevant to the system analyzed here can be found in the asymmetric chiral phosphoric acid-catalyzed oxetane opening developed by Sun and co-workers, which relies on the controlled hydrolysis of a silyl chloride to generate HCl.[19] We considered whether HBr generated by the hydrolysis of TMSBr could account for the observed variability in reaction performance. Using the enantioselective conversion of 3-phenyloxetane (**2**) to trimethylsilyl-protected bromohydrin **3** as a model reaction, we tested this hypothesis through the controlled introduction of HBr into the reaction medium. High levels of enantioselectivity were maintained in the presence of catalytic levels of HBr,[20] but reaction rates were increased by over an order of magnitude compared to the reaction carried out with the rigorous exclusion of HBr (Figure 3A/Table S1).[21,22]

The positive rate dependence on added proton sources suggested that HBr—rather than TMSBr—could be the active reagent in the oxetane-opening reaction. Consistent with that hypothesis, stoichiometric quantities of squaramide **1a** were shown to mediate the reaction of oxetane **2** with HBr[23] to afford bromohydrin **4** in 98% e.e. (Figure 3B). In addition, **1a** proved effective as a catalyst (2 mol % loading) for the opening of **2** with HCl, affording the chlorohydrin analogue of **4** in 92% e.e. at 4 °C (Figure S42).[24] Taken together, these results implicate a mechanism involving cocatalysis by **1a** and HBr wherein enantioselective oxetane ring opening by HBr is followed by silylation of bromohydrin **4** by TMSBr to afford **3** and regenerate HBr.

The identification of the HBr cocatalyed mechanism accounts for the variation of rate with reaction scale given that adventious water is expected to be present in greater ratios in small-scale reactions. However, it does not provide a satisfactory explanation for the irreproducible enantioselectivies observed with suboptimal catalysts (Figure 2C). Provided temperature is well controlled, variability in enantioselectivity is indicative of competing reaction mechanisms. The obvious candidate for such a competing pathway would be the racemic,

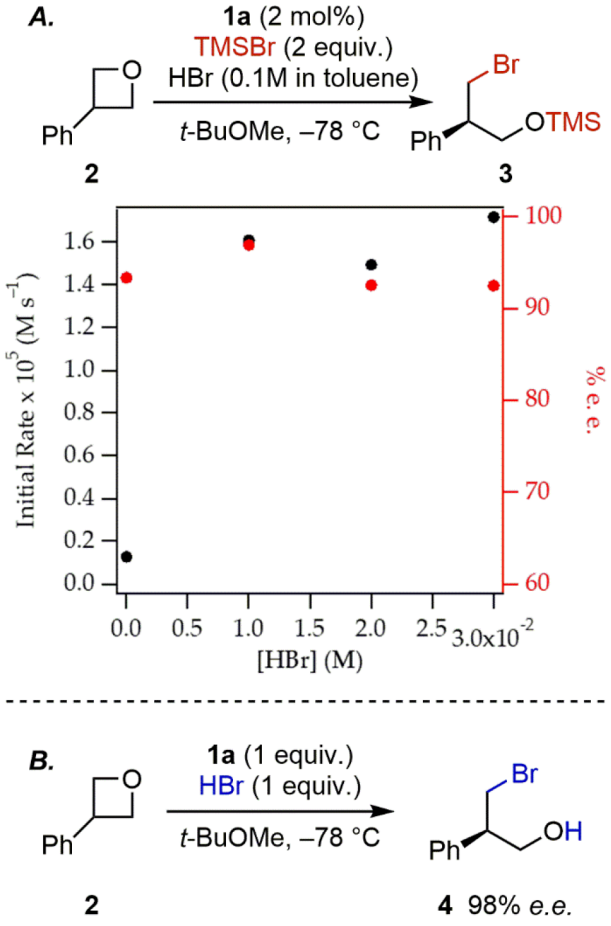

Figure 3. (A) Effect of HBr (generated by the photochemical reaction of Br_2 in toluene) on reaction rate (black dots) and enantioselectivity (red dots) ([**1a**] = 0.002 M, $[\mathbf{2}]_0$ = 0.1 M, $[TMSBr]_0$ = 0.2 M). The reaction with [HBr] = 0 was conducted in the presence of $TMSCHN_2$ as a base (see text). Reaction rates were determined via *in situ* FTIR monitoring using a ReactIR (see General Procedure for ReactIR experiments in the Supporting Information). (B) Enantioselective addition of HBr to **2** promoted by **1a**.

uncatalyzed ring-opening addition of HBr to the oxetane. However, under the relevant, low [HBr] reaction conditions, the uncatalyzed reaction is very slow and cannot account for the observed variability in e.e. (Figure S48). Thus, the data are most consistent with competing catalytic mechanisms being involved, and we hypothesized that the originally proposed silyl-Lewis-acid mechanism might also be operative. To test this possibility, we sought to identify a base that could completely suppress the HBr pathway without interfering with the activity of the HBD catalyst. The additive had to be selected carefully, because salts introduced either as anionic bases or as the conjugate acids of neutral bases are generally strong inhibitors of anion-binding pathways due to competitive association to the hydrogen-bond-donor active site.[25] Gratifyingly, trimethylsilyldiazomethane, which has previously been demonstrated to function as a noninterfering base in hydrogen-bond-donor catalyzed cation-olefin cyclizations,[9p] was found to neutralize HBr rapidly and quantiatively without any deleterious effect on the squaramide catalyst under the standard reaction conditions (Figure 4A). In the presence of $TMSCHN_2$ the reaction of oxetane **2** with TMSBr was observed to proceed at appreciable rates but more slowly and with similar levels of enantioselectivity relative to the HBr-*co*-

https://doi.org/10.1021/jacs.1c03992
J. Am. Chem. Soc. 2021, 143, 9585−9594

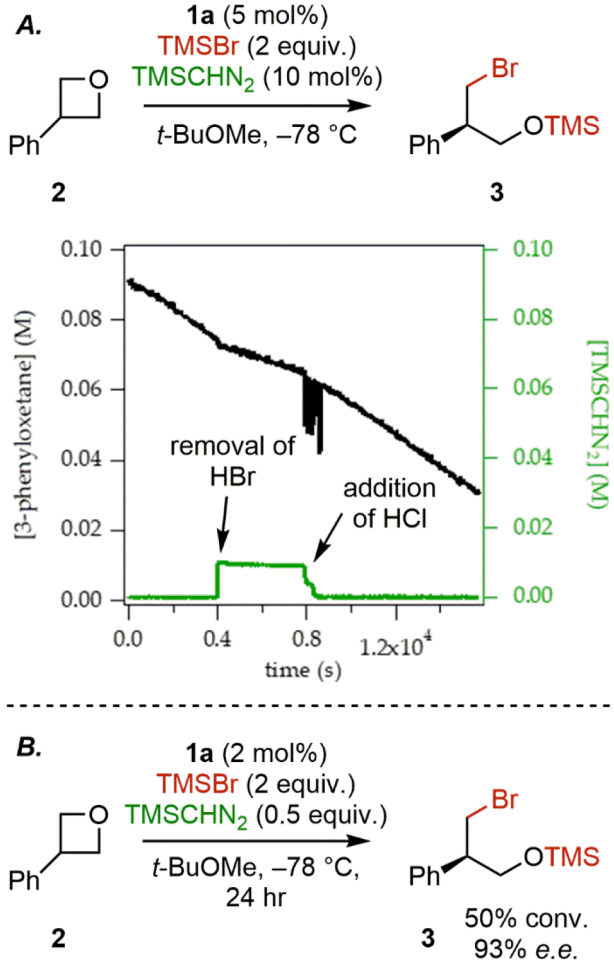

Figure 4. (A) Reaction time-course measured using *in situ* FTIR monitoring. Upon the addition of $TMSCHN_2$ (green ~4000 s), the rate of consumption of **2** (black) decreases but continues at a lowered rate. Upon the addition of HCl (8000 s), the $TMSCHN_2$ is rapidly consumed. Following complete consumption of $TMSCHN_2$ the rate of oxetane consumption increases. (B) The reaction run in the presence of $TMSCHN_2$ proceeds with high enantioselectivity and at a rate that is slower but still competitive with the HBr cocatalyzed pathway.

catalyzed reaction (Figure 4B). A distinct TMSBr-mediated reaction must therefore be operative alongside the HBr cocatalyzed pathway, with both pathways contributing to the formation of product **3** with high levels of enantioenrichment in the presence of catalyst **1a**. Moreover, this phenomenon is not limited to model oxetane **2**. A survey of the **1a**-catalyzed opening of **2** and 6 additional oxetanes selected to represent the diversity of the originally reported reaction scope (3-aryl, 3-alkyl, 3-heteratomic, and 3,3-disubstituted oxetanes) revealed an average difference of <5% e.e. between the two mechanisms.[26]

The observations outlined above and extensive ground state and kinetic analyses conducted in the absence (Figures S9, S12–S24) and presence (Figures S36–S41) of added $TMSCHN_2$ are consistent with a scenario in which the two catalytic mechanisms outlined in Figure 6A are operating simultaneously in the **1a**-catalyzed ring-opening addition of TMSBr to oxetanes. In the Lewis-acid pathway, which is the only pathway operative in the presence of $TMSCHN_2$, kinetic analysis revealed a first-order dependence on the concentrations of squaramide **1a**, oxetane **2**, and TMSBr, which is consistent with rate-determining oxetane ring-opening via bromide addition.[27] In the absence of $TMSCHN_2$, both the Lewis-acid and Brønsted-acid pathways are operative. Under these conditions and at steady-state,[28] a first-order dependence on TMSBr, a first-order dependence on [**1a**], and a positive order in [**2**] with a nonzero y-intercept are observed. The positive order in [**2**] can be ascribed to contribution of the Lewis-acid pathway, while the nonzero intercept reflects a zeroth-order dependence on [**2**] for the Brønsted-acid pathway. On the basis of the combination of this zeroth-order dependence and positive orders for TMSBr, **1a**, and HBr concentrations (Figure 3A), the alcohol silylation step that affords **3** with regeneration of the squaramide-HBr complex[29] is proposed to be rate-determining in the Brønsted acid pathway. A primary kinetic isotope effect was observed in a one-pot competition experiment between unlabeled and 2,4-$^{13}C_2$-**2** in the presence of $TMSCHN_2$ (see Supporting Information for details). Taken together with the previously reported[91] primary KIE observed in an analogous experiment in the absence of $TMSCHN_2$, we conclude that bromide delivery is enantiodetermining for both mechanisms.

The recognition that two distinct catalytic pathways are operative in the enantioselective oxetane-opening reaction catalyzed by **1a** enabled the successful development of a scalable protocol. In the case of substrate **2**, the challenge of reproducibly achieving optimal rates without compromising enantioselectivity can be met by maximizing the HBr-*co*-catalyzed pathway, without participation of the racemic uncatalyzed reaction which intervenes at high [HBr] (Figure 3A).[30] The conversion of 1 g of **2** to **3** was thus achieved in 89% yield and 97% e.e. using 1 mol % of **1a** and 6.5 mol % added H_2O (Figure 5). Catalyst **1a** was reisolated from the reaction in 90% yield and displayed undiminished activity and enantioselectivity in a subsequent reaction (Figure S6).

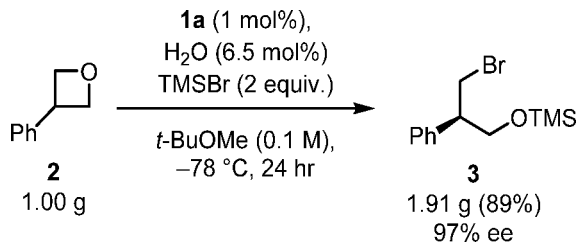

Figure 5. Addition of trace water allows for high reactivity and enantioselectivity with reduced loadings of squaramide **1a** in a gram-scale reaction of oxetane **2** with TMSBr.

The enantiodetermining ring-opening transition states for the Brønsted and Lewis acid pathways were modeled computationally in order to assess the catalyst features responsible for high stereocontrol in both pathways (complete computational details and computational references are provided in the SI). In the Brønsted acid cocatalyzed pathway, $\mathbf{TS}_{protic}$-***R*** and $\mathbf{TS}_{protic}$-***S*** were identified as the lowest energy transition states leading to the major and minor product enantiomers (Figure 6B). $\mathbf{TS}_{silyl}$-***R*** and $\mathbf{TS}_{silyl}$-***S*** were the lowest energy enantiomeric transition states located for the Lewis acid pathway (Figure 6C). The computational model was validated by comparison of predicted and measured enantioselectivity for a series of chiral catalysts with varied aryl pyrrolidine fragments (Figure 7). Although the computational models

https://doi.org/10.1021/jacs.1c03992
J. Am. Chem. Soc. 2021, 143, 9585–9594

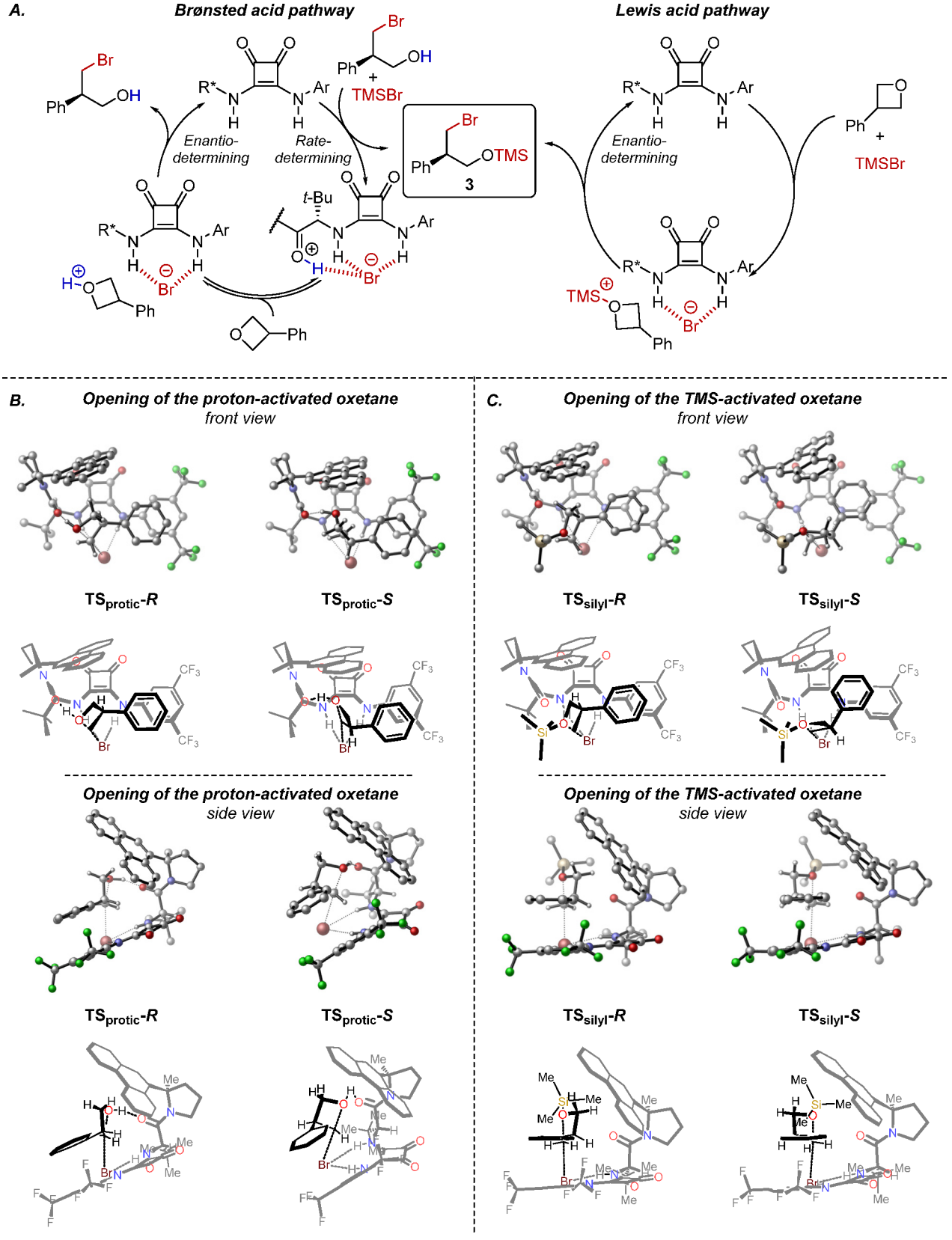

Figure 6. (A) Proposed reaction mechanisms consisting of competing Brønsted and Lewis acid pathways. (B) Computed lowest energy major (*R*) and minor (*S*) transition states for the Brønsted acid pathway ($\Delta\Delta E^{\ddagger}$ = 2.6 kcal/mol). (C) Computed lowest energy major (*R*) and minor (*S*) transition states for the Lewis acid pathway ($\Delta\Delta E^{\ddagger}$ = 2.5 kcal/mol). Transition states were optimized at SMD (Et_2O) − B97D/def2-SVP. The electronic energies were corrected by single-point refinement at SMD (Et_2O) − B97D3/def2-TZVP.

https://doi.org/10.1021/jacs.1c03992
J. Am. Chem. Soc. 2021, 143, 9585−9594

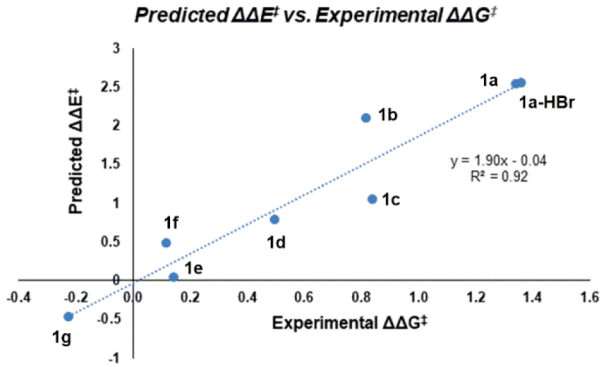

Figure 7. Predicted $\Delta\Delta E^{\ddagger}$ vs experimental $\Delta\Delta G^{\ddagger}$ for the Lewis acid pathways for catalysts **1a**−**1g** and the Brønsted acid pathway for catalyst **1a**. See Figure 8 for catalyst structures, Table S11 for tabulated data, and Figures S7 and S34 for experimental details.

overestimate the magnitude of the enantioselectivities, the model reproduces the trends in the data (R^2 = 0.92) including the inversion in the sense of enantioinduction for the Lewis acid pathway with catalyst **1g**.[31]

Qualitative analysis of $\mathbf{TS_{silyl}}$-***R*** and $\mathbf{TS_{silyl}}$-***S*** reveals significant similarity between the two transition structures: in both, the forming C−Br and breaking C−O bonds are positioned almost identically relative to the catalyst, and the two transition structures can be overlaid to a significant degree (Figure S63). However, the developing α-silyloxy methylene group, which is predicted to bear much of the positive electrostatic potential (Figure S62), is positioned differently in the two structures. In $\mathbf{TS_{silyl}}$-***R***, this methylene group points toward the amide and the 9-phenanthryl substituent of the catalyst, in an ideal orientation for stabilizing cation-π and cation-dipole interactions.[32] In contrast, the methylene is oriented away from the arene and amide in $\mathbf{TS_{silyl}}$-***S***, resulting in attenuated stabilizing interactions relative to those in the major pathway. In the Brønsted acid pathway, additional conformational constraint is provided by a hydrogen-bonding interaction between the protonated oxetane and the amide. This interaction can be readily accommodated in the transition state leading to the major enantiomer, such that the position and conformation of the oxetane as it undergoes ring opening in the catalyst active site is similar in $\mathbf{TS_{silyl}}$-***R*** and $\mathbf{TS_{protic}}$-***R***, allowing the cation-π interaction to be maintained. However, in $\mathbf{TS_{protic}}$-***S***, maintenance of the anchoring H-bond requires the disrupting of the rest of the network of interactions between the catalyst and substrate, including the proposed cation-π interaction.

The computationally derived hypothesis that cation-π interactions play a critical role in enantioinduction was tested experimentally by evaluating the extended series of aryl-pyrrolidinosquaramides **1a**−**1g** in the reactions of **2** with TMSBr and HBr (Figure 8A). In consistency with the models, selectivity for the *R*-enantiomer in both pathways was observed to correlate with the ability of the aryl substituent to engage in a cation-π interaction, with electron-deficient or less polarizable arenes affording decreased selectivity for the *R*-enantiomer.[32,33] Furthermore, all catalysts induced higher selectivity for the *R*-product in the HBr cocatalyzed reactions of **2** relative to the Lewis acid pathway, consistent with the proposed reinforcing hydrogen-bonding interaction in the Brønsted acid mechanism. The results in Figure 8A,B also provide a clear explanation for why enantioselectivities under

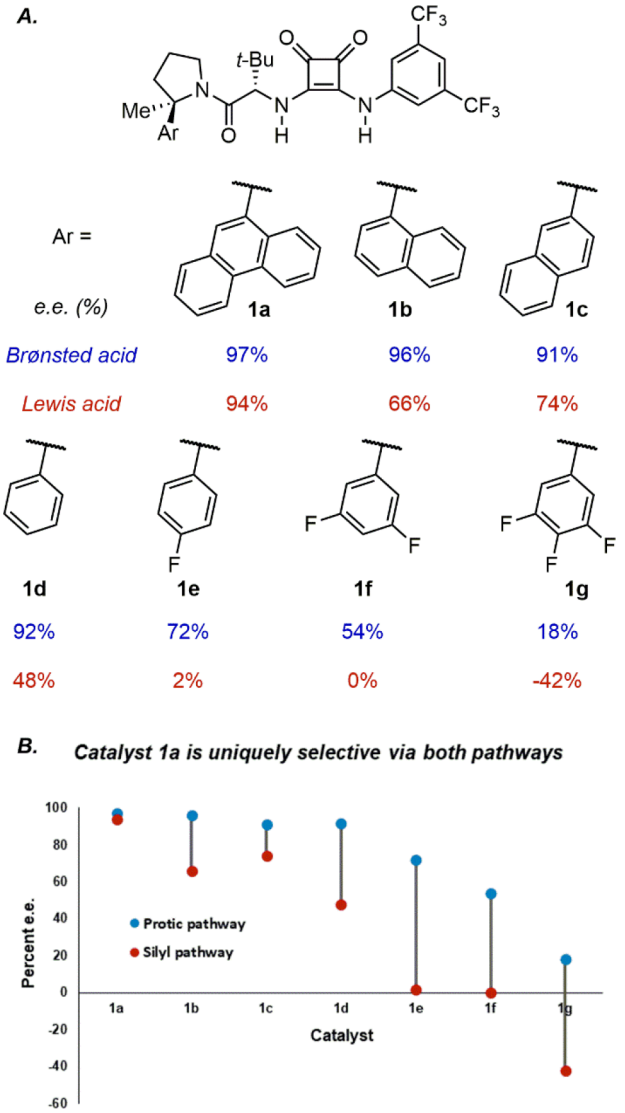

Figure 8. (A) Enantioselectivity for the reaction of **2** catalyzed by **1a**−**1g** determined both for the HBr-promoted reaction and with TMSBr in the presence of $TMSCHN_2$ (average of two runs, see Figures S7 and S33 for details). (B) Graphical representation of relative enantioselectivities of the Brønsted and Lewis acid mechanisms for reactions of **2** catalyzed by **1a**−**1g**.

the original screening conditions were more consistent with catalyst **1a** than with less selective catalysts (Figure 2C): squaramide **1a** is the only catalyst tested that is highly enantioselective for both the Brønsted acid and the Lewis acid pathways, with every other catalyst showing large differences in e.e. or even favoring alternate enantiomers of product for the two pathways. Under the original reaction conditions employed for the catalyst optimization studies—in which the concentration of HBr was not controlled carefully—both pathways are kinetically competent and therefore contribute significantly to product formation. As the optimization experiments were designed, only a catalyst that is highly enantioselective for both mechanisms can generate product in consistently high e.e.'s.

The fact that catalyst **1a** induces high enantioselectivity across different mechanisms in the oxetane ring-opening is intriguing and touches on the broader phenomenon of privileged chiral catalysts.[4a] The electrostatic potential map

https://doi.org/10.1021/jacs.1c03992
J. Am. Chem. Soc. 2021, 143, 9585−9594

of **1a** (Figure 9A) reveals an electron-rich pocket (in red) defined by the amide and 9-phenanthryl substituent positioned

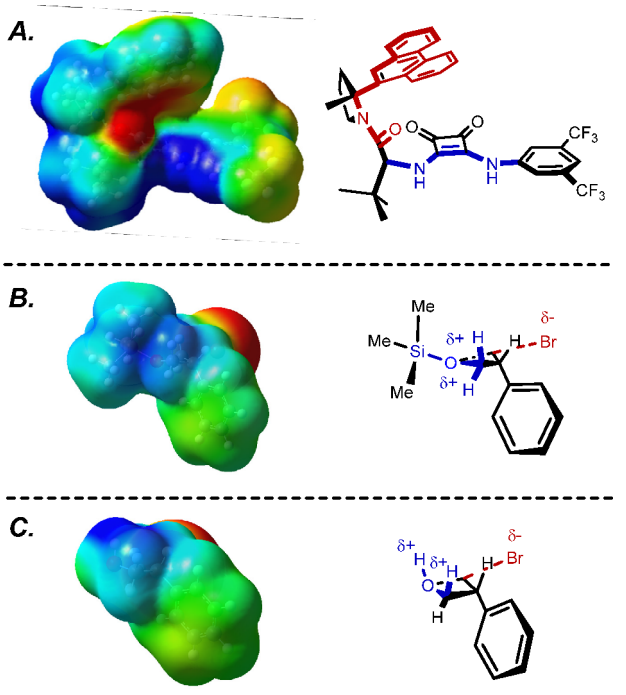

Figure 9. (A) Electrostatic potential map of catalyst **1a** using the geometry from $\mathbf{TS}_{\mathbf{silyl}}$-***R*** (scale from −0.03 to +0.03). (B) Electrostatic potential map of the Lewis acid transition state using the geometry from $\mathbf{TS}_{\mathbf{silyl}}$-***R*** (scale from −0.06 to +0.06). (C) Electrostatic potential map of the Brønsted acid transition state using the geometry from $\mathbf{TS}_{\mathbf{protic}}$-***R*** (scale from −0.06 to +0.08). All ESPs were computed at SMD (Et2O) − B97-D3/Def2-TZVP and plotted with a density isovalue of 0.0004.

adjacent to the H-bond donor motif (in blue). While the protonated and silylated transition states in the oxetane opening present dramatically different steric features, they possess dipoles that display charge similarly within the catalyst active site (Figure 9B,C). The precise nature (i.e., cation-π, charge-dipole, H-bonding) and relative strengths of the stabilizing interactions differ between the two pathways (see Figure S67 and S68 for a detailed analysis), but through cooperation between the arene and the amide, the catalyst can stabilize positive charge in the major transition states to a significant degree from both the protonated and the silylated oxetane. The presence of multiple, reinforcing sites for secondary interactions may be a general feature of privileged scaffolds that underlies their ability to stabilize or destabilize a diverse range of transition states.

CONCLUSION

Given the intrinsic challenges associated with attaining stereocontrol with small-molecule catalysts, observation of high enantioselectivity might, in principle, be taken as evidence of a "well behaved" transformation that proceeds through a single mechanistic pathway (or an ensemble of closely related transition states) rather than through distinct, completing mechanisms.[34] The unexpected discovery detailed here, that the squaramide-catalyzed ring opening of oxetanes with TMSBr proceeds through competing Lewis- and Brønsted-acid reaction pathways, adds to a growing body of evidence[35] that high enantioselectivity can be manifested despite the availability of distinct mechanistic pathways to the same product. It is noteworthy that the participation of competing mechanisms remained unrecognized throughout the course of our reaction development and scope studies, only becoming apparent upon scale-up efforts and subsequent careful mechanistic analysis. Thus, in optimizing enantioselectivity in the oxetane opening, we unwittingly optimized a catalyst for generality across two different mechanisms. Caution should of course be exercised before attempting to draw general conclusions from a specific case study such as this one, but given that detailed mechanistic investigations of new asymmetric reactions rarely if ever precede catalyst optimization efforts, such scenarios could be more common than is generally appreciated. Given the truism that "you get what you screen for,"[36] this study raises the intriguing question of whether the discovery of remarkably general chiral catalysts over the past several decades might be tied in part to the optimization of reactions that are not always "well behaved."

ASSOCIATED CONTENT

Supporting Information

The Supporting Information is available free of charge at https://pubs.acs.org/doi/10.1021/jacs.1c03992.

Procedures and analytical data for enantioselective reactions, details of mechanistic studies, and computational studies (PDF)

AUTHOR INFORMATION

Corresponding Author

Eric N. Jacobsen − *Department of Chemistry and Chemical Biology, Harvard University, Cambridge, Massachusetts 02138, United States;* orcid.org/0000-0001-7952-3661; Email: jacobsen@chemistry.harvard.edu

Authors

Daniel A. Strassfeld − *Department of Chemistry and Chemical Biology, Harvard University, Cambridge, Massachusetts 02138, United States*

Russell F. Algera − *Department of Chemistry and Chemical Biology, Harvard University, Cambridge, Massachusetts 02138, United States*

Zachary K. Wickens − *Department of Chemistry and Chemical Biology, Harvard University, Cambridge, Massachusetts 02138, United States;* orcid.org/0000-0002-5733-5288

Complete contact information is available at: https://pubs.acs.org/10.1021/jacs.1c03992

Notes

The authors declare no competing financial interest.

ACKNOWLEDGMENTS

Financial support for this work was provided by the NIH through GM043214 and a postdoctoral fellowship to Z.K.W.

REFERENCES

(1) (a) Knowles, W. S. Asymmetric Hydrogenations (Nobel Lecture). *Angew. Chem., Int. Ed.* **2002**, *41*, 1998−2007. For an authoritative historical perspective, see: (b) Kagan, H. B. in *Comprehensive Asymmetric Catalysis*. Jacobsen, E. N.; Pfaltz, A.;

Yamamoto, H., Eds., Springer: New York, 1999; Vol. *1*, Ch. 1, pp 9−30.

(2) Some notable examples: (a) Gao, Y.; Klunder, J. M.; Hanson, R. M.; Masamune, H.; Ko, S. Y.; Sharpless, K. B. Catalytic asymmetric epoxidation and kinetic resolution: modified procedures including in situ derivatization. *J. Am. Chem. Soc.* **1987**, *109*, 5765−5780. (b) Kolb, H. C.; VanNieuwenhze, M. S.; Sharpless, K. B. Catalytic Asymmetric Dihydroxylation. *Chem. Rev.* **1994**, *94*, 2483−2547. (c) Corey, E. J.; Helal, C. J. Reduction of Carbonyl Compounds with Chiral Oxazaborolidine Catalysts: A New Paradigm for Enantioselective Catalysis and a Powerful New Synthetic Method. *Angew. Chem., Int. Ed.* **1998**, *37*, 1986−2012. (d) Noyori, R.; Takeshi, O. Asymmetric Catalysis by Architectural and Functional Molecular Engineering: Practical Chemo- and Stereoselective Hydrogenation of Ketones. *Angew. Chem., Int. Ed.* **2001**, *40*, 40−73. (e) Schaus, S. E.; Brandes, B. D.; Larrow, J. F.; Tokunaga, M.; Hansen, K. B.; Gould, A. E.; Furrow, M. E.; Jacobsen, E. N. Highly Selective Hydrolytic Kinetic Resolution of Terminal Epoxides Catalyzed by Chiral (salen)Cobalt(III)-Complexes. Practical Synthesis of Enantioenriched Terminal Epoxides and 1,2-Diols. *J. Am. Chem. Soc.* **2002**, *124*, 1307−1315.

(3) (a) Finn, M. G.; Sharpless, K. B. Mechanism of asymmetric epoxidation. 2. Catalyst structure. *J. Am. Chem. Soc.* **1991**, *113*, 113−126. (b) Ford, D. D.; Nielsen, L. P. C.; Zuend, S. J.; Musgrave, C. B.; Jacobsen, E. N. Mechanistic Basis for High Stereoselectivity and Broad Substrate Scope in the (salen)Co(III)-Catalyzed Hydrolytic Kinetic Resolution. *J. Am. Chem. Soc.* **2013**, *135*, 15595−15608.

(4) (a) Yoon, T. P.; Jacobsen, E. N. Privileged chiral catalysts. *Science* **2003**, *299*, 1691−1693. Intriguingly, a similar phenomenon has been noted in enzymatic catalysis, wherein particular protein folds appear to be particularly well suited for catalyzing mechanistically distinct reactions: (b) Anantharaman, V.; Aravind, L.; Koonin, E. V. Emergence of diverse biochemical activities in evolutionarily conserved structural scaffolds of proteins. *Curr. Opin. Chem. Biol.* **2003**, *7*, 12−20.

(5) In the arena of asymmetric hydrogenation in particular, it is common to rely on known chiral ligand scaffolds for the identification of new applications. For a highly noteworthy, but representative example, see: Hansen, K. B.; Hsiao, Y.; River, N.; Clausen, A.; Kubryk, M.; Krska, S.; Rosner, T.; Simmons, B.; Balsells, J.; Ikemoto, N.; Sun, Y.; Spindler, F.; Malan, C.; Grabowski, E. J. J.; Armstrong, J. D., III Highly Efficient Asymmetric Synthesis of Sitagliptin. *J. Am. Chem. Soc.* **2009**, *131*, 8798−8804.

(6) (a) Jacobsen, E. N. Asymmetric Catalysis of Epoxide Ring-Opening Reactions. *Acc. Chem. Res.* **2000**, *33*, 421−431. For two recent examples, see: (b) Salehi Marzijarani, N.; Lam, Y.-h.; Wang, X.; Klapars, A.; Qi, J.; Song, Z.; Sherry, B. D.; Liu, Z.; Ji, Y. New Mechanism for Cinchona Alkaloid-Catalysis Allows for an Efficient Thiophosphorylation Reaction. *J. Am. Chem. Soc.* **2020**, *142*, 20021−20029. (c) Yamashita, Y.; Noguchi, A.; Fushimi, S.; Hatanaka, M.; Kobayashi, S. Chiral Metal Salts as Ligands for Catalytic Asymmetric Mannich Reactions with Simple Amides. *J. Am. Chem. Soc.* **2021**, *143*, 5598−5604.

(7) For example, the landmark advances by the Krische and Buchwald groups on enantioselective C−C and C−heteroatom bond-forming reactions have relied almost entirely on chiral ligands developed for asymmetric hydrogenation: (a) Kim, S. W.; Zhang, W.; Krische, M. J. Catalytic Enantioselective Carbonyl Allylation and Propargylation via Alcohol-Mediated Hydrogen Transfer: Merging the Chemistry of Grignard and Sabatier. *Acc. Chem. Res.* **2017**, *50*, 2371−2380. (b) Liu, R. Y.; Buchwald, S. L. CuH-Catalyzed Olefin Functionalization: From Hydroamination to Carbonyl Addition. *Acc. Chem. Res.* **2020**, *53*, 1229−1243.

(8) Whitesell, J. K. C_2 Symmetry and Asymmetric Induction. *Chem. Rev.* **1989**, *89*, 1581−1590.

(9) For examples of enantiocontrol via addition of neutral nucleophiles to cationic sp^2 electrophiles, see: (a) Reisman, S. E.; Doyle, A. G.; Jacobsen, E. N. Enantioselective thiourea-catalyzed additions to oxocarbenium ions. *J. Am. Chem. Soc.* **2008**, *130*, 7198−7199. (b) Knowles, R. R.; Lin, S.; Jacobsen, E. N. Enantioselective thiourea-catalyzed cationic polycyclizations. *J. Am. Chem. Soc.* **2010**, *132*, 5030−5032. (c) Bergonzini, G.; Schindler, C. S.; Wallentin, C.-J.; Jacobsen, E. N.; Stephenson, C. R. J. Photoredox activation and anion binding catalysis in the dual catalytic enantioselective synthesis of *β*-amino esters. *Chem. Sci.* **2014**, *5*, 112−116. (d) Yeung, C. S.; Ziegler, R. E.; Porco, J. A., Jr.; Jacobsen, E. N. Thiourea-catalyzed enantioselective addition of indoles to pyrones: alkaloid cores with quaternary carbons. *J. Am. Chem. Soc.* **2014**, *136*, 13614−13617. (e) Banik, S. M.; Levina, A.; Hyde, A. M.; Jacobsen, E. N. Lewis acid enhancement by hydrogen-bond donors for asymmetric catalysis. *Science* **2017**, *358*, 761−764. (f) Attard, J. W.; Osawa, K.; Guan, Y.; Hatt, J.; Kondo, S.-I.; Mattson, A. Silanediol anion binding and enantioselective catalysis. *Synthesis* **2019**, *51*, 2107−2115. (g) Andres, R.; Wang, Q.; Zhu, J. Asymmetric total synthesis of (−)-arborisidine and (−)-19-*epi*-arborisidine enabled by a catalytic enantioselective Pictet−Spengler reaction. *J. Am. Chem. Soc.* **2020**, *142*, 14276−14285. (h) Ronchi, E.; Paradine, S. M.; Jacobsen, E. N. Enantioselective, Catalytic Multicomponent Synthesis of Homoallylic Amines Enabled by Hydrogen-Bonding and Dispersive Interactions. *J. Am. Chem. Soc.* **2021**, *143*, 7272−7278. For examples of enantiocontrol via addition of neutral nucleophiles to cationic sp^3 electrophiles, see: (i) Lin, S.; Jacobsen, E. N. Thiourea-catalyzed ring opening of episulfonium ions with indole derivatives by means of stabilizing non-covalent interactions. *Nat. Chem.* **2012**, *4*, 817−824. (j) Zhang, H.; Lin, S.; Jacobsen, E. N. Enantioselective selenocyclization via dynamic kinetic resolution of seleniranium ions by hydrogen-bond donor catalysts. *J. Am. Chem. Soc.* **2014**, *136*, 16485−16488. For examples of catalysis via enantioselective anion delivery, see: (k) Birrell, J. A.; Desrosiers, J.-N.; Jacobsen, E. N. Enantioselective acylation of silyl ketene acetals through fluoride anion-binding catalysis. *J. Am. Chem. Soc.* **2011**, *133*, 13872−13875. (l) Strassfeld, D. A.; Wickens, Z. K.; Picazo, E.; Jacobsen, E. N. Highly Enantioselective, Hydrogen-Bond-Donor Catalyzed Additions to Oxetanes. *J. Am. Chem. Soc.* **2020**, *142*, 9175−9180. For examples proceeding via enantioselective proton transfer, see: (m) Metternich, J. B.; Reiterer, M.; Jacobsen, E. N. Asymmetric Nazarov cyclizations of unactivated dienones by hydrogen-bond-donor/Lewis acid co-catalyzed enantioselective proton-transfer. *Adv. Synth. Catal.* **2020**, *362*, 4092−4097. (n) Momo, P. B.; Leveille, A. N.; Farrar, E. H. E.; Grayson, M. N.; Mattson, A. E.; Burtoloso, A. C. B. Enantioselective S−H insertion reactions of *α*-carbonyl sulfoxonim ylides. *Angew. Chem., Int. Ed.* **2020**, *59*, 15554−15559. For examples proceeding via enantioselective concerted substitutions, see: (o) Bendelsmith, A. J.; Kim, S. C.; Wasa, M.; Roche, S. P.; Jacobsen, E. N. Enantioselective synthesis of *α*-allyl amino esters via hydrogen-bond-donor catalysis. *J. Am. Chem. Soc.* **2019**, *141*, 11414−11419. (p) Kutateladze, D. A.; Strassfeld, D. A.; Jacobsen, E. N. Enantioselective Tail-to-Head Cyclizations Catalyzed by Dual-Hydrogen-Bond Donors. *J. Am. Chem. Soc.* **2020**, *142*, 6951−6956. For examples of enantiocontrol through direct electrophile activation via LUMO lowering, see: (q) Cruz-Acosta, F.; de Armas, P.; Garcia-Tellado, F. Water-compatible hydrogen-bond activation: a scaleable and organocatalytic model for the stereoselective multicomponent aza-Henry reaction. *Chem. - Eur. J.* **2013**, *19*, 16550−16554. (r) Lykke, L.; Carlsen, B. D.; Rambo, R. S.; Jørgensen, K. A. Catalytic asymmetric synthesis of 4-nitropyrazolidines: an access to optically active 1,2,3-triamines. *J. Am. Chem. Soc.* **2014**, *136*, 11296−11299. (s) Liu, R. Y.; Wasa, M.; Jacobsen, E. N. Enantioselective synthesis of tertiary *α*-chloro esters by non-covalent catalysis. *Tetrahedron Lett.* **2015**, *56*, 3428−3430.

(10) (a) Dolling, U.-H.; Davis, P.; Grabowski, E. J. J. Efficient Catalytic Asymmetric Alkylations. 1. Enantioselective Synthesis of (+)-Indacrinone via Chiral Phase-Transfer Catalysis. *J. Am. Chem. Soc.* **1984**, *106*, 446−447. (b) Studer, M.; Blaser, H.-U.; Exner, C. Enantioselective Hydrogenation Using Heterogeneous Modified Catalysts: An Update. *Adv. Synth. Catal.* **2003**, *345*, 45−65. (c) Tian, S.-K.; Chen, Y.; Hang, J.; Tang, L.; McDaid, P.; Deng, L. Asymmetric Organic Catalysis with Modified Cinchona Alkaloids. *Acc. Chem. Res.* **2004**, *37*, 621−631. (d) Marcelli, T.; Hiemstra, H. Cinchona Alkaloids in Asymmetric Organocatalysis. *Synthesis* **2010**,

https://doi.org/10.1021/jacs.1c03992
J. Am. Chem. Soc. 2021, 143, 9585−9594

2010, 1229−1279. (e) Jew, S.-s.; Park, H.-g. *Cinchona*-based phase-transfer catalysts for asymmetric synthesis. *Chem. Commun.* **2009**, 7090−7103. (f) *Cinchona Alkaloids in Synthesis and Catalysis: Ligands, Immobilization and Organocatalysis*; Song, C. E., Ed.; Wiley-VCH Verlag GmbH & Co. KGaA: 2009. (g) Genov, G. R.; Douthwaite, J. L.; Lahdenpera, A. S. K.; Gibson, D. C.; Phipps, R. J. Enantioselective remote C−H activation directed by a chiral cation. *Science* **2020**, *367*, 1246−1251.

(11) Wendlandt, A. E.; Vangal, P.; Jacobsen, E. N. Quaternary stereocenters via an enantioconvergent catalytic SN1 reaction. *Nature* **2018**, *556*, 447−451.

(12) For a recent study examining the potential role of hidden proton catalysis with silyl Lewis acids see: Schmidt, R. K.; Muther, K.; Muck-Lichtenfeld, C.; Grimme, S.; Oestreich, M. Silylium ion-catalyzed challenging Diels-Alder reactions: the danger of hidden proton catalysis with strong Lewis acids. *J. Am. Chem. Soc.* **2012**, *134*, 4421−4428.

(13) The topic of Lewis acid vs Brønsted acid catalysis has been extensively investigated in the context of transformations mediated by Lewis acidic metal salts with weakly coordinating counterions. For notable examples, see: (a) Wabnitz, T. C.; Yu, J.-Q.; Spencer, J. B. Evidence that protons can be the active catalysts in Lewis acid mediated hetero-Michael addition reactions. *Chem. - Eur. J.* **2004**, *10*, 484−493. (b) Rosenfeld, D. C.; Shekhar, S.; Takemiya, A.; Utsunomiya, M.; Hartwig, J. F. Hydroamination and hydroalkoxylation catalyzed by triflic acid. Parallels to reactions initiated with metal triflates. *Org. Lett.* **2006**, *8*, 4179−4182. (c) Li, Z.; Zhang, J.; Brouwer, C.; Yang, C.-G.; Reich, N. W.; He, C. Brønsted Acid Catalyzed Addition of Phenols, Carboxylic Acids, and Tosylamdies to Simple Olefins. *Org. Lett.* **2006**, *8*, 4175−4178. (d) Liu, P. N.; Zhou, Z. Y.; Lau, C. P. The Lewis Acidic Ruthenium-Complex-Catalyzed Addition of β-Diketones to Alcohols and Styrene Is in Fact Brønsted Acid Catalyzed. *Chem. - Eur. J.* **2007**, *13*, 8610−8619. (e) Tschan, M. J.-L.; Thomas, C. M.; Strub, H.; Carpentier, J.-F. Copper(II) Triflate as a Source of Triflic Acid: Effective, Green Catalysis of Hydroalkoxylation Reactions. *Adv. Synth. Catal.* **2009**, *351*, 2496−2504. (f) Bowring, M. A.; Bergman, R. G.; Tilley, T. D. Disambiguation of metal and Brønsted acid catalyzed pathways for hydroarylation with platinum(II) catalysts. *Organometallics* **2011**, *30*, 1295−1298. (g) Dang, T. T.; Boeck, F.; Hintermann, L. Hidden Brønsted Acid Catalysis: Pathways of Accidntal or Deliberate Generation of Triflic Acid from Metal Triflates. *J. Org. Chem.* **2011**, *76*, 9353−9361. (h) McKinney Brooner, R. E.; Widenhoefer, R. A. Stereochemistry and Mechanism of the Brønsted Acid Catalyzed Intramolecular Hydrofunctionalization of an Unactivated Cyclic Alkene. *Chem. - Eur. J.* **2011**, *17*, 6170−6178. For some recent examples see: (i) Munz, D.; Webster-Gardiner, M.; Fu, R.; Strassner, T.; Goddard, W. A., III; Gunnoe, T. B. Proton or Metal? The H/D Exchange of Arenes in Acidic Solvents. *ACS Catal.* **2015**, *5*, 769−775. (j) Chen, J.; Goforth, S. K.; McKeown, B. A.; Gunnoe, T. B. Brønsted acid-catalyzed intramolecular hydroamination of unactivated alkenes: metal triflates as an *in situ* source of triflic acid. *Dalton Trans.* **2017**, *46*, 2884−2891. (k) Sletten, E. T.; Tu, Y.-J.; Schlegel, H. B.; Nguyen, H. M. Are Brønsted Acids the True Promoter of Metal-Triflate-Catalyzed Glycosylations? A Mechnistic Probe into 1,2-*cis*-Aminoglycoside Formation by Nickel Triflate. *ACS Catal.* **2019**, *9*, 2110−2123. For reviews see: (l) Hashmi, A. S. K. Homogeneous gold catalysis: The role of protons. *Catal. Today* **2007**, *122*, 211−214. (m) Taylor, J. G.; Adrio, L. A.; Hii, K. K. Hydroamination reactions by metal triflates: Brønsted acid vs. metal catalysis? *Dalt. Trans.* **2010**, *39*, 1171−1175.

(14) (a) Sammakia, T.; Latham, H. A. On the use of ferrocenyl cations as chiral Lewis acids: evidence for protic acid catalysis. *Tetrahedron Lett.* **1995**, *36*, 6867−6870. (b) Denmark, S. E.; Barsanti, P. A.; Wong, K.-T.; Stavenger, R. A. Enantioselective Ring Opening of Epoxides with Silicon Tetrachloride in the Presence of a Chiral Lewis Base. *J. Org. Chem.* **1998**, *63*, 2428−2429. (c) Hu, G.; Huang, L.; Huang, R. H.; Wulff, W. D. Evidence for a Boroxinate Based Brønsted Acid Derivative of VAPOL as the Active Catalyst in the Catalytic Asymmetric Aziridination Reaction. *J. Am. Chem. Soc.* **2009**, *131*, 15615−15617.

(15) The opposite phenomenon—the generation of Lewis acidic derivatives of chiral Brønsted acids and their potential role as active catalysts in enantioselective transformations—has been investigated more extensively. For examples of ostensibly chiral-acid catalyzed reaction where silyl Lewis acid derivatives of the conjugate base were demonstrated to be the active catalysts see ref 16. For examples of ostensibly chiral-acid catalyzed reactions where Lewis acidic metal salts of the conjugate base were demonstrated to be the active catalysts see ref 17. For examples of chiral-acid catalyzed reactions where Lewis acid derivatives are shown to be less active and/or less enantioselective see ref 18.

(16) (a) Rowland, E. B.; Rowland, G. B.; Rivera-Otero, E.; Antilla, J. C. Brønsted Acid-Catalyzed Desymmetrization of *meso*-Aziridines. *J. Am. Chem. Soc.* **2007**, *129*, 12084−12085. (see also ref 17d for a follow-up study) (b) Garcia-Garcia, P.; Lay, F.; Garcia-Garcia, P.; Rabalakos, C.; List, B. A Powerful Chiral Counteranion Motif for Asymmetric Catalysis. *Angew. Chem., Int. Ed.* **2009**, *48*, 4363−4366. (c) Zamfir, A.; Tsogoeva, S. B. Asymmetric Hydrocyanation of Hydrazones Catalyzed by in Situ Formed *O*-Silylated BINOL-Phopshate: A Convenient Access to Versatile α-Hydrazino Acids. *Org. Lett.* **2010**, *12*, 188−191. (d) Gatzenmeier, T.; van Gemmeren, M.; Xie, Y.; Höfler, D.; Leutzsch, M.; List, B. Asymmetric Lewis acid organocatalysis of the Diels-Alder reaction by a silylated C-H acid. *Science* **2016**, *351*, 949−952. For a review covering the application of silylated chiral disulfonimide catalysts see: (e) James, T.; van Gemmeren, M.; List, B. Development and Applications of Disulfonimides in Enantioselective Organocatalysis. *Chem. Rev.* **2015**, *115*, 9388−9409.

(17) (a) Hatano, M.; Moriyama, K.; Maki, T.; Ishihara, K. Which is the Actual Catalyst: Chiral Phosphoric Acid or Chiral Calcium Phopshate? *Angew. Chem., Int. Ed.* **2010**, *49*, 3823−3826. (b) Rueping, M.; Bootwicha, T.; Sugiono, E. Chiral Brønsted Acids and Their Calcium Salts in Catalytic Asymmetric Mannich Reactions of Cyclic 1,3-Diketones. *Synlett* **2011**, *2011*, 323−326. (c) Zheng, W.; Zhang, Z.; Kaplan, M. J.; Antilla, J. C. Chiral Calcium VAPOL Phosphate Mediated Asymmetric Chlorination and Michael Reactions of 3-Substituted Oxindoles. *J. Am. Chem. Soc.* **2011**, *133*, 3339−3341. (d) Della Sala, G. Studies on the true catalyst in the phosphate-promoted desymmetrization of *meso*-aziridines with silylated nucleophiles. *Tetrahedron* **2013**, *69*, 50−56. (e) Terada, M.; Kanomata, K. Metal-Free Chiral Phopshoric Acid or Chiral Metal Phosphate as Active Catalyst in the Activation of *N*-Acyl Aldimines. *Synlett* **2011**, *2011*, 1255−1258. (f) Alix, A.; Lalli, C.; Retailleau, P.; Masson, G. Hihgly Enantioselective Electrophilic α-Bromination of Enecarbamates: Chiral Phosphoric Acid and Calcium Phopshate Salt Catalysts. *J. Am. Chem. Soc.* **2012**, *134*, 10389−10392. (g) Lebee, C.; Blanchard, F.; Masson, G. Highly Enantioselective Intermolecular Iodo- and Chloroamination of Enecarbamates Catalyzed by Chiral Phosphoric Acids or Calcium Phosphate Salts. *Synlett* **2016**, *27*, 559−563.

(18) (a) Hasegawa, A.; Naganawa, Y.; Fushimi, M.; Ishihara, K.; Yamamoto, H. Design of Brønsted Acid-Assisted Chiral Brønsted Acid Catalyst Bearing a Bis(triflyl)methyl Group for a Mannich-Type Reaction. *Org. Lett.* **2006**, *8*, 3175−3178. (b) Cheon, C. H.; Yamamoto, H. *N*-Triflylthiophosphoramide Catalyzed Enantioselective Mukaiyama Aldol Reaction of Aldehydes with Silyl Enol Ethers of Ketones. *Org. Lett.* **2010**, *12*, 2476−2479. (c) Rueping, M.; Theissmann, T.; Kuenkel, A.; Koenigs, R. M. Highly Enantioselective Organocatalytic Carbonyl-Ene Reaction with Strongly Acidic, Chiral Brønsted Acids as Efficient Catalysts. *Angew. Chem., Int. Ed.* **2008**, *47*, 6798−6801. (d) Klussmann, M.; Ratjen, L.; Hoffmann, S.; Wakchaure, V.; Goddard, R.; List, B. Synthesis of TRIP and Analysis of Phosphate Salt Impurities. *Synlett* **2010**, *2010*, 2189−2192. (e) Gheewala, C. D.; Collins, B. E.; Lambert, T. H. An aromatic ion platfom for enantioselective Brønsted acid catalysis. *Science* **2016**, *351*, 961−965.

https://doi.org/10.1021/jacs.1c03992
J. Am. Chem. Soc. 2021, 143, 9585−9594

(19) Yang, W.; Wang, Z.; Sun, J. Enantioselective oxetane ring opening with chloride: unusual use of wet molecular sieves for the controlled release of HCl. *Angew. Chem., Int. Ed.* **2016**, *55*, 6954−6958.
(20) See also notes 13 and 21 in ref 9l, as well as Figures S6 and S7 in the Supporting Information of ref 9l.
(21) $TMSCHN_2$ was found to be uniquely effective at quenching HBr rapidly without generating any byproducts that interfered with the catalytic reaction. For additional details, see Figures 4 and S30−S32. For a previous report of the use of $TMSCHN_2$ as a noninterfering base in H-bond-donor catalysis, see ref 9p.
(22) A similar rate and e.e. profile is produced with HBr generated by the addition of *i*-PrOH to TMSBr (Figure S2). The reaction rate is also depressed slightly at increased concentrations of added *i*-PrOH (>3 × 10−2 M). No such inhibitory effect on rate is observed for HBr generated from Br_2 and toluene. For additional experiments probing this effect see Figures S51-S53.
(23) Generated as an anhydrous solution in toluene through the photochemical reaction of Br_2 and toluene, see General Procedure C in the Supporting Information for additional information.
(24) In contrast to HBr, at 4 °C HCl does not react with oxetane **2** at an appreciable rate in the absence of an H-bond donor catalyst.
(25) Raheem, I. T.; Thiara, P. S.; Peterson, E. A.; Jacobsen, E. N. Enantioselective Pictet-Spengler-Type Cyclizations of Hydroxylactams: H-Bond Donor Catalysis by Anion Binding. *J. Am. Chem. Soc.* **2007**, *129*, 13404−13405.
(26) While the HBr cocatalyzed pathway is more enantioselective for 3-phenyloxetane (**2**) this was not true for all substrates. For some substrates, the TMSBr pathway was found to be more enantioselective, providing further evidence for a *bona fide* silyl Lewis acid pathway (see Figures S8 and S35).
(27) Alternatively, rate-determining TMSBr heterolysis with nucleophilic assistance by the oxetane cannot be ruled out on the basis of the kinetic data. However, this proposal would require that silyl transfer between **2**-Me_3Si^+ and **2** is rapid relative to reversion to the starting materials (i.e., TMSBr heterolysis is irreverisble) and that the former process is rapid relative to bromide delivery to **2**-Me_3Si^+ to account for the ^{13}C KIE observed for the silyl pathway in one-pot competition experiments.
(28) At the start of the reaction the resting state is the squaramide-HBr complex. In the first turnover, the HBr is consumed and the steady-state regime depicted in Figure 6A is established. As consumption of **2** approaches completion, the concentration of **2** will be much lower than that of TMSBr, because TMSBr is used in excess. Consequently, the resting state can shift back to the catalyst-HBr complex at high conversion. For a detailed discussion see Figure S10.
(29) Studies of catalyst **1a**, the **1a**-HBr complex, the corresponding urea and thiourea, and their HBr complexes using *in situ* infrared spectroscopy support the depicted structure wherein the *t*-leucine amide is protonated by HBr. This is also supported by computational modelling and comparisons between predicted and measured IR spectra, which indicate a bridging interaction between the protonated amide and the squaramide-bound bromide. See Figures S15-S17 for a detailed discussion.
(30) With substrates for which the Lewis-acid pathway affords higher levels of enantioselectivity than the Brønsted-acid pathway (see Note. Twenty-six and Figures S8 and S35), reactions run on larger scale are expected to provide product in higher levels of e.e. than reactions run on screening scale and the addition of a proton source is anticipated to be detrimental to enantioselectivity. The slow rate of the uncatalyzed reaction at low [HBr] (Figure S48) allows an alternate tactic for accelerating large-scale reactions of substrates where the Lewis-acid pathway is more enantioselective: rather than adding a proton source, the concentration of the reaction can be increased. This approach was successfully implemented for the gram-scale synthesis of pretomanid detailed in ref 9l. Prior to scaling up reactions of interest, the relative enantioselectivities of the two pathways for any substrate of interest should first be determined by comparing the results obtained on screening scale using General Procedure C and General Procedure D (detailed in the Supporting Information).
(31) Overestimation of computed enantioselectivities in these types of correlations is common: (a) Schneebeli, S. T.; Hall, M. L.; Breslow, R.; Friesner, R. Quantitative DFT Modeling of the Enantiomeric Excess for Dioxirane-Catalyzed Epoxidations. *J. Am. Chem. Soc.* **2009**, *131*, 3965−3973. (b) Zuend, S. J.; Jacobsen, E. N. Mechanism of Amido-Thiourea Catalyzed Enantioselective Imine Hydrocyanation: Transition State Stabilization via Multiple Non-Covalent Interactions. *J. Am. Chem. Soc.* **2009**, *131*, 15358−15374. (c) Uyeda, C.; Jacobsen, E. N. Transition State Charge Stabilization Through Multiple Non-Covalent Interactions in the Guanidinium-Catalyzed Enantioselective Claisen Rearrangement. *J. Am. Chem. Soc.* **2011**, *133*, 5062−5075.
(32) (a) Mecozzi, S.; West, A. P.; Dougherty, D. A. Cation-π interactions in simple aromatics: electrostatics provide a predictive tool. *J. Am. Chem. Soc.* **1996**, *118*, 2307−2308. (b) Ma, J. C.; Dougherty, D. A. The cation-π interaction. *Chem. Rev.* **1997**, *97*, 1303−1324. (c) Kennedy, C. R.; Lin, S.; Jacobsen, E. N. The cation-π interaction in small-molecule catalysis. *Angew. Chem., Int. Ed.* **2016**, *55*, 12596−12624. (d) Neel, A. J.; Hilton, M. J.; Sigman, M. S.; Toste, F. D. Exploiting non-covalent π interactions for catalyst design. *Nature* **2017**, *543*, 637−646. (e) Yamada, S. Cation-π Interactions in Organic Synthesis. *Chem. Rev.* **2018**, *118*, 11353−11432.
(33) These data offer a striking contrast to those obtained in an H-bond-donor catalyzed multicomponent synthesis of chiral homoallylic amines (ref 9h.), where (poly)fluorinated phenyl substituents on the aryl pyrrolidine moiety of the catalyst provided *higher* levels of enantioselectivity than phenylpyrrolidine. In that transformation, differential stabilization by dispersive π-stacking interactions, rather than differential cation-π interactions, were concluded to contribute to enantioinduction.
(34) Indeed, the participation of competing catalyzed pathways—rather than poor enantioinduction in a single pathway—may underlie poor performance in many asymmetric catalytic reactions. For an example where a Brønsted-acid pathway was demonstrated to be deleterious to enantioselectivity in a Lewis-acid-catalyzed reaction, necessitating the use of freshly distilled $SiCl_4$, see ref 14b. See also: (a) Denmark, S. E.; Fan, Y.; Eastgate, M. D. Lewis Base Catalyzed, Enantioselective Aldol Addition of Methyl Trichlorosilyl Ketene Acetal to Ketones. *J. Org. Chem.* **2005**, *70*, 5235−5248. (b) Fu, H.; Look, G. C.; Zhang, W.; Jacobsen, E. N.; Wong, C.-H. Mechanistic Study of a Synthetically Useful Monooxygenase Model Using the Hypersensitive Probe *trans*-2-Phenyl-1-vinylcyclopropane. *J. Org. Chem.* **1991**, *56*, 6497−6500. Mitigation of the effects of competing catalytic pathways, when recognized, is typically addressed through modification of the reaction conditions (ref 18a) or through catalyst redesign to suppress the poorly enantioselective pathway. See for example: (c) Denmark, S. E.; Fu, J. On the Mechanism of Catalytic, Enantioselective Allylation of Aldehydes with Chlorosilanes and Chiral Lewis Bases. *J. Am. Chem. Soc.* **2000**, *122*, 12021−12022.
(35) A recent study of flexible, peptide-based catalysts provides evidence of how the transition state ensembles in enantioselective reactions can include significant structural diversity: Crawford, J. M.; Stone, E. A.; Metrano, A. J.; Miller, S. J.; Sigman, M. S. Parametrization and Analysis of Peptide-Based Catalysts for the Atroposelective Bromination of 3-Arylquinazolin-4(3*H*)-ones. *J. Am. Chem. Soc.* **2018**, *140*, 868−871.
(36) Schmidt-Dannert, C.; Arnold, F. H. Directed evolution of industrial enzymes. *Trends Biotechnol.* **1999**, *17*, 135−136.

https://doi.org/10.1021/jacs.1c03992
J. Am. Chem. Soc. 2021, 143, 9585−9594